Cysteine-Scanning Mutagenesis of Transmembrane Segment 1 of Glucose Transporter GLUT1: Extracellular Accessibility of Helix Positions†

Matthias Heinze, Ingrid Monden, and Konrad Keller*

Institute of Pharmacology, Freie Universität Berlin, Thielallee 67-73, D-14195 Berlin, FRG

Received July 23, 2003; Revised Manuscript Received October 19, 2003

ABSTRACT: Transmembrane segment 1 of the cysteine-less GLUT1 glucose transporter was subjected to cysteine-scanning mutagenesis. The majority of single-cysteine mutants were functional transporters, as assessed by 2-deoxy-D-glucose uptake or 3-*O*-methyl-D-glucose transport. Substitution of cysteine for Leu-21, Gly-22, Ser-23, Gln-25, and Gly-27, however, led to uptake rates that were less than 10% of that of the nonmutated cysteine-less GLUT1. NEM, a membrane-permeable agent, was used to identify positions that are sensitive to transport alteration by sulfhydryl reagents, whereas uptake modification by the membrane-impermeant pCMBS indicated accessibility to water-soluble solutes from the external cell environment. Twelve of the 21 single-cysteine mutants were significantly ($p < 0.01$) affected by NEM, and on the basis of this sensitivity, four positions were identified by pCMBS to form a water-accessible surface within helix 1. The pCMBS-sensitive positions are localized at the exofacial C-terminal end along a circumference of the helix.

All known members of the extended GLUT family (SLC2A) belong to a major superfamily (*1*) whose members facilitate the transfer of water-soluble solutes across the membrane lipid bilayer. The GLUT transporters have a predicted basic structure of 12 putative transmembrane segments (TMs)[1] and, except for a subset of GLUTs, designated class III transporters (*2*), have a large extracellular glycosylated loop between TM1 and TM2. In an attempt to create a general model for the tertiary arrangement of transmembrane segments that is valid for all members of the facilitator group, transmembrane domains 1, 2, 4, 5, 7, 8, 10, and 11 have been postulated to possess properties consistent with their role as a part of the translocation pathway (*3*). With respect to GLUT1, probably the most intensively studied isoform of the GLUT family, transmembrane segments 3, 5, 7, 8, and 11 have been identified as the most amphipathic helices due to the distribution of hydrophilic and hydrophobic amino acid residues (*4*). Because no high-resolution structure of any member of the GLUT family is available and unequivocal knowledge of transporter tertiary or quaternary structure does not exist, various models of the membrane helical packing arrangement have been proposed (*5*−*10*). Transmembrane segment 1 (TM1) has received particular consideration in Widdas' theoretical assignment (*8*) since it exists as an α-helix at an aqueous interface of the predicted translocation pathway which together with transmembrane domains 7 and 12 is involved in the opening of a canonical cleft during glucose transfer through the membrane. In a three-dimensional (3D) structural prediction based on molecular modeling, Fischbarg and co-workers (*10*) suggest that GLUT1 contains two channels; the first includes TM7, -8, and -11 as crucial components forming the "main" channel for glucose transport, whereas the second "auxiliary" channel involves helices 1−3 and 7. Recently, the reported crystal structures of two bacterial transporters, the lactose permease (*11*) and the glycerol 3-phosphate transporter (*12*), indicate that helix 1 is integrated in a pore-forming helical bundle.

Probing the structure at putative pore regions of GLUT1, cysteine-scanning mutagenesis in conjunction with the application of sulfhydryl agents was successfully applied to helices 2 (*13*), 5 (*14*), 7 (*13*, *15*), 10 (*16*), and 11 (*17*). This substituted-cysteine-accessibility method (*18*), which has been used to characterize the structures of numerous integral membrane proteins, probes the environment of any amino acid residue by mutating it to cysteine and by determining the reaction of introduced cysteines with sulfhydryl reagents. In GLUT1, two thiol reagents, parachloromercuribenzenesulfonate (pCMBS) and *N*-ethylmaleimide (NEM), have been chosen to provide valuable structural information. pCMBS is a membrane-impermeant thiol reagent that reacts selectively and reversibly with protein cysteine residues and, when applied at the extracellular side of the plasma membrane, reports on protein positions that can be accessed from the extracellular environment. NEM is a membrane-permeable sulfhydryl reagent that covalently reacts with thiol groups and, on the basis of transport modification, provides information about the sensitivity of a particular helix position. Since it has been reported by independent groups (*19*−*21*) that GLUT1 devoid of its six native cysteine residues has a near-normal activity (from >100 to 77% of that of wild-type GLUT1), it is likely that the global structure of a cysteine-less GLUT1 is the same as that of wild-type GLUT1. In

† This work was supported by Grants Ke390/6-2 and Ke390/6-3 from the Deutsche Forschungsgemeinschaft.

* To whom correspondence should be addressed. Telephone: +49 30 84451873. Fax: +49 30 84451818. E-mail: kellerfu@zedat.fu-berlin.de.

[1] Abbreviations: NEM, *N*-ethylmaleimide; pCMBS, parachloromercuribenzenesulfonate; 2-DOG, 2-deoxy-D-glucose; 3-OMG, 3-*O*-methyl-D-glucose; TM, transmembrane segment.

10.1021/bi030175w CCC: $27.50
Published on Web 12/31/2003

each of the helices that have been investigated, substituted cysteines appear to be reliable indicators of sensitivity and accessibility of the wild-type residues, for which they are substituted. The aim of this study was to identify by cysteine-scanning mutagenesis and sulfhydryl sensitivity scanning those positions in TM1 that are sensitive to extracellular sulfhydryl reagents. In the case of pCMBS, our data indicate that amino acid residues in the outer part of the exofacial half are accessible to water-soluble solutes. This finding is in line with those membrane models that predict that TM1 is integrated in a helix bundle that forms the translocation pathway.

EXPERIMENTAL PROCEDURES

Mutagenesis. A 1523 bp *Bam*HI−*Bst*YI fragment of the human GLUT1 cDNA derived from pSPGT (*22*) was subcloned into a *Bgl*II site of the *Xenopus* oocyte expression vector pSP64T (*23*), leading to the 5716 bp-containing plasmid pSP64T-GLUT1. This construct served as a template for generation of a Cys-less GLUT1 cDNA that encodes a functional glucose transporter (*20*). A set of 21 mutant cDNAs encoding single-cysteine-containing GLUT1 transporters at positions 13−33 in TM1 was obtained by site-directed mutagenesis using the QuikChange site-directed mutagenesis kit (Strategene Europe, Amsterdam, The Netherlands). Mutants were checked by restriction fragment analysis and were finally confirmed by DNA sequence analysis (ABI PRISM DNA sequencer connected to a McIntosh computer).

cRNA Preparation and Microinjection. In vitro synthesis of capped cRNA was conducted with plasmid templates of the *Xba*I-linearized mutants and wild-type GLUT1 using the in vitro transcription protocol provided by AMBION (mMESSAGE mMACHINE, Ambion, Austin, TX). The amount of transcribed cRNA was calculated by counting radioactivity of incorporated [^{35}S]thioUTP and by calculating the A_{260}/A_{280} ratio. In addition, cRNA integrity was checked on a gel. For each preparation, the concentrations of cRNAs were adjusted to values of ~0.5 mg/mL. Fifty nanoliters of cRNA was injected into *Xenopus* oocytes which 24 h earlier had been manually isolated from ovarian lobes. Details of collection, defolliculation, and culture of *Xenopus* oocytes as well as of cRNA microinjection have been described previously (*24*, *25*).

Western Dot Blot Analysis and Confocal Laser Scanning Microscopy. Plasma membrane fractions were prepared according to the procedure by Keller et al. (*24*) with a slight modification (*25*). Western dot blot analyses were performed as described previously (*26*, *27*) using the chemiluminescent detection kit for horseradish peroxidase (Applichem, Darmstadt, FRG). The first antibody (AK 1462) was used at a 1:750 dilution; the anti-rabbit IgG (whole molecule) peroxidase-conjugated second antibody, developed in goat (Sigma, St. Louis, MO), was diluted 1:1500. Finally, 5, 10, 25, 50, and 75 ng of purified GLUT1 (a kind gift from G. Lienhard, Hanover, NH) served as standards for the comparison of signal intensities.

Preparations of *Xenopus* oocytes for confocal microscopy images were made as described previously (*13*) with the modification that the fixed oocytes were frozen and cut into halves using a standard freezing microtome. Oocyte halves were treated with an anti-GLUT1 antibody raised against the final 15 C-terminal amino acids (AK 1462, 20 μg/mL) followed by the second FITC-conjugated goat anti-rabbit IgG antibody (Sigma, diluted 1:400 in PBS and 2% horse serum). Fluorescence intensities were recorded in the line scan mode by scanning the fluorescence over the plasma membrane area and peripheral parts of the cytoplasm. The fluorescence was scanned through a depth of 10 μm along a line drawn from outside the plasma membrane up to 50 μm into the cell interior. For each oocyte half, fluorescence intensities were recorded along three separate lines. The intensities over the plasma membrane area were averaged and divided by the average fluorescence over the cytoplasm. The ratios (R) (mean ± the standard error of the mean calculated from three oocytes) indicated plasma membrane targeting of a mutant transporter compared with Cys-less GLUT1.

Determination of Transport Activity, Sensitivity, and Accessibility. Tritium-labeled 2-deoxy-D-glucose (50 μM, 1 μCi/0.5 mL transport assay, 30 min uptake time) or 3-*O*-methyl-D-glucose (1 mM, 5 μCi/0.5 mL transport assay, 5 min transport time) was used for uptake or transport assessment following a standard protocol described previously (*13*). Uptake or transport values of water-injected *Xenopus* oocytes (sham) were always subtracted. Since the absolute uptake or transport values can vary considerably with different batches of *Xenopus* oocytes, both the relative basal transport activity and the remaining activity after application of pCMBS or NEM of a particular mutant-expressing single oocyte were calculated as follows:

$$\text{relative basal activity (\%)} = \frac{\text{Xi}_{\text{mutant}} - \text{mean}_{\text{sham}}}{\sum(\text{Xi}_{\text{Cys-less GLUT1}} - \text{mean}_{\text{sham}})/n} \times 100$$

or

$$\text{remaining activity (\%)} = \frac{\text{Xi}_{\text{mutant plus inhibitor}} - \text{mean}_{\text{sham plus inhibitor}}}{\sum(\text{Xi}_{\text{mutant minus inhibitor}} - \text{mean}_{\text{sham minus inhibitor}})/n} \times 100$$

The lipid-soluble membrane-permeable reagent NEM (10 mM, preincubation for 30 min before 3-OMG transport) was used to test the sensitivity of a particular cysteine position within the helix with respect to transport alteration. The membrane-impermeant reagent pCMBS (1 mM, preincubation for 30 min before 2-DOG uptake) was used to identify those helix positions that are accessible to solutes from the extracellular aqueous phase. Standard protocols for determination of transport activity in *Xenopus* oocytes, lysis of oocytes, and measurement of radioactivity were presented previously (*24*). Statistical evaluation was performed using UltraFit (Biosoft, Cambridge, U.K.).

Materials. The HPLC-purified oligonucleotides for cysteine-scanning mutagenesis were obtained from Sigma (Taufkirchen, FRG). The radiolabeled glucose analogues (2-[1,2-^{3}H]deoxy-D-glucose, concentration of 37 MBq/mL, specific activity of 876.9 GBq/mmol; and 3-*O*-[*methyl*-^{3}H]-D-glucose, concentration of 37 MBq/mL, specific activity of 2.3 TBq/mmol) were purchased from Perkin-Elmer Life Science, Inc. (Boston, MA). The substances 2-deoxy-D-

Table 1: 2-DOG Uptake Rates of Single-Cysteine Mutants Relative to That of Cys-less GLUT1[a]

% of that of Cys-less GLUT1		% of that of Cys-less GLUT1	
endofacial PM side			
M13C	80 ± 27	L24C	62 ± 27
L14C	105 ± 22	Q25C	7 ± 10
A15C	79 ± 26	F26C	102 ± 25
V16C	115 ± 26	G27C	6 ± 7
G17C	104 ± 32	Y28C	20 ± 14
G18C	87 ± 26	N29C	86 ± 26
A19C	36 ± 22	T30C	70 ± 21
V20C	121 ± 32	G31C	126 ± 42
L21C	4 ± 6	V32C	73 ± 29
G22C	9 ± 7	I33C	57 ± 17
S23C	5 ± 8	exofacial PM side	

[a] Tritium-labeled 2-DOG uptake was assessed in *Xenopus* oocytes expressing each of the 21 single-cysteine mutants. Uptake rates in water-injected oocytes were always subtracted. Groups of 10−15 oocytes were included in the transport assay, and 2-DOG uptake rates of single oocytes were expressed as a percentage of the mean uptake of cysteine-less GLUT1 (for details, see Experimental Procedures). The relative rate of 2-DOG uptake of a particular mutant (mean ± the standard deviation) was calculated from five to nine separate experiments.

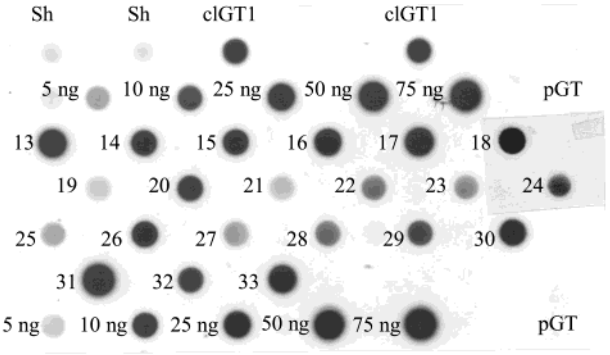

FIGURE 1: Western dot blot analysis of single-cysteine mutants. Plasma membrane (PM) fractions of water-injected *Xenopus* oocytes (Sh) and oocytes expressing Cys-less GLUT1 (clGT1) or the 21 single-cysteine mutants (designated by their position) were prepared for immunoblot analysis; 5, 10, 25, 50, and 75 ng of purified GLUT1 glucose transporter (pGT, a kind gift from G. Lienhard) were applied as a standard, and 5 μg of PM protein was loaded per mutant. Rabbit antiserum raised against the final 15 C-terminal amino acid residues was used as a first antibody (AK 1462, diluted 1:750), and an anti-rabbit peroxidase-conjugated goat IgG (1:1500) was the second antibody.

glucose, 3-*O*-methyl-D-glucose, collagenase type I, and *N*-ethylmaleimide were from Sigma; 4-(chloromercuri)-benzenesulfonic acid, sodium salt, was from Toronto Research Chemicals (North York, ON). Hybond ECL nitrocellulose membrane was obtained from Amersham Bioscience Europe GmbH (Freiburg, FRG). Female *Xenopus laevis* frogs were from African Xenopus Facility CC (Knysna, Republic of South Africa).

RESULTS

Basal Transport Activities and Expression of Single-Cysteine Mutants. Twenty-one amino acid residues, which according to the widely accepted secondary structure model of GLUT1 (*4*) form TM1 of the Cys-less GLUT1 glucose transporter, were replaced, one at a time, by site-directed mutagenesis with cysteine to create single-cysteine mutant transporters. On the basis of a near-normal function of the Cys-less GLUT1 (*20*), the change of a native amino acid residue with cysteine provides information about the importance of the side chain at a particular helix position. Table 1 documents how cysteine-scanning mutagenesis affects Cys-less GLUT1 transport activity relative to the control, as assessed by 2-deoxy-D-glucose uptake in *Xenopus* oocytes. The majority of injected cRNAs translated into functional transporters, allowing the investigation of single-cysteine mutants with respect to sensitivity to sulfhydryl reagents and accessibility to external water-soluble solutes. Five mutants (L21C, G22C, S23C, Q25C, and G27C) exhibited marginal transport activities, which were less than 10% of that of the nonmutated Cys-less GLUT1.

To investigate plasma membrane expression, Western dot blot analysis was performed from plasma membrane fractions of *Xenopus* oocytes collected and processed according to a standard protocol (*24*, *25*). Figure 1 demonstrates that a few cysteine mutants, i.e., A19C, L21C, S23C, Q25C, and G27C, exhibited considerably lower levels of plasma membrane expression of the transporter protein than Cys-less GLUT1. In the case of L21C, S23C, Q25C, or G27C, this correlates with 2-DOG uptake rates of less than 10% of that of Cys-less GLUT1. Figure 2 presents representative confocal microscopy images and line plots of the relative fluorescence intensities recorded over the plasma membrane area and the adjacent cytoplasm of an oocyte half. The calculated ratios (*R*) give the mean intensities (arbitrary units) obtained from three randomly selected *Xenopus* oocytes, each scanned at three separate lines. In Cys-less GLUT1, the relative fluorescence signal over the plasma membrane was 8 times higher than the average over the cytoplasm, and is comparable with the previously published ratio for wild-type GLUT1 (*27*). In the five indicated single-cysteine mutants, the ratios were much less than 8, suggesting that substitution of a cysteine impairs plasma membrane targeting of the mutant transport proteins.

Sulfhydryl Group Sensitivity Scanning. Table 2 summarizes our data on 2-deoxy-D-glucose (2-DOG) uptake in the presence of pCMBS and 3-*O*-methyl-D-glucose (3-OMG) transport after NEM application. Preincubation and uptake and transport assessment followed a standard protocol, as published previously (*13*). Sulfhydryl reagent-induced alterations in transport activity are presented as the percent uptake or transport of untreated controls (see Experimental Procedures). As pCMBS slowly dissociates from its thiol binding site, transport assays always included the sulfhydryl reagents at the indicated concentrations. Because NEM inhibits hexokinase activity (*28*), the transport assay used 3-OMG as a glucose analogue that unlike 2-DOG is transported but not phosphorylated upon entry into the cell. NEM consistently inhibited the Cys-less GLUT1-mediated transport in *Xenopus* oocytes [remaining activity, 82 ± 20% (mean ± the standard deviation)]. In some of the mutants, no uptake or transport activity could be measured after subtraction of the value of sulfhydryl reagent-treated water-injected *Xenopus* oocytes (marked nd). If basal transport activities were reasonably high, inhibition of uptake or transport clearly indicated "sensitivity" to sulfhydryl reagents and in the case of pCMBS also "accessibility" to water-soluble solutes from the external environment. Conversely,

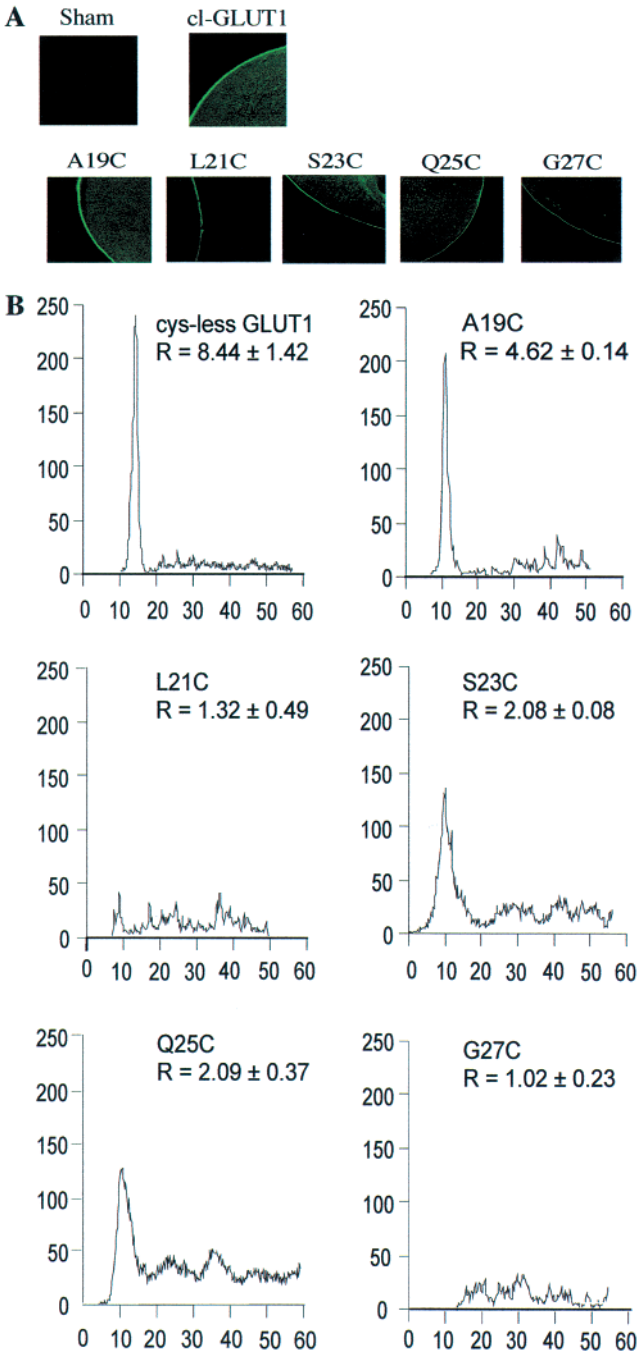

FIGURE 2: Confocal microscopy images (A) and line plots (B) of selected single-cysteine mutants. In cut oocyte halves, the fluorescence was scanned through a depth of 10 μm. Oocyte halves were treated with an anti-GLUT1 antibody raised against the final 15 C-terminal amino acids (AK 1462, 20 μg/mL) followed by the second FITC-conjugated goat anti-rabbit IgG antibody (Sigma catalog no. F-0511, diluted 1:400 in PBS and 2% horse serum). In the line scan mode, fluorescence labeling was measured at three separate locations per oocyte half of three randomly selected *Xenopus* oocytes per group. In the line plots, the *y*-axis presents the relative fluorescence intensity in arbitrary units and the *x*-axis gives the distance in micrometers. *R* is the ratio of the relative fluorescence intensity over the plasma membrane area to that over the cytoplasm (mean ± the standard error of the mean).

mutants with marginal basal transport activities were not reliable indicators (mutants marked with an asterisk) and thus have been omitted from the helical wheel representation.

Data in Table 2 demonstrate that according to statistical criteria ($p < 0.01$) 12 of 21 mutants were affected by NEM with 11 showing transport inhibition and one at position 33 (I33C) displaying an increase in transport activity. Transport was largely unaffected for the majority of single-cysteine mutants in the pCMBS-treated group. Four positions at the exoplasmic end of helix 1 were accessible to pCMBS and, as a general consequence, can react with water-soluble solutes from the extracellular fluid. It is interesting to note that both pCMBS and NEM caused uptake or transport stimulation after reaction with cysteine at position 33. Helical wheel representations in Figure 3 show that positions that can react with a membrane-permeable reagent like NEM are located around helix circumferences through the entire plasma membrane thickness. More importantly, all identified pCMBS-accessible positions are located at a circumference at the exofacial end of helix 1.

Table 2: 3-OMG Transport or 2-DOG Uptake of Single-Cysteine Mutants in the Presence of Extracellular NEM or pCMBS Relative to Untreated Controls[a]

mutant	% NEM application activity	no. of oocytes	% pCMBS application activity	no. of oocytes	S	A
M13C	75 ± 11	63	110 ± 33	59	+	
L14C	94 ± 12	80	109 ± 22	64		
A15C	nd	75	99 ± 21	37	+	
V16C	5 ± 3	77	107 ± 34	40	+	
G17C	99 ± 13	79	117 ± 41	67		
G18C	3 ± 3	76	116 ± 27	64	+	
A19C	nd	67	107 ± 52	36	+	
V20C	68 ± 14	78	116 ± 20	84	+	
L21C	34 ± 45	79	nd	91	*	*
G22C	47 ± 57	72	92 ± 71	78	*	
S23C	13 ± 23	79	52 ± 51	82	*	
L24C	78 ± 30	87	120 ± 20	55		
Q25C	nd	57	nd	63	*	*
F26C	5 ± 4	78	99 ± 16	78	+	
G27C	nd	81	nd	102	*	*
Y28C	52 ± 41	53	104 ± 69	61	+	
N29C	81 ± 21	68	122 ± 24	60		
T30C	1 ± 1	64	nd	62	+	+
G31C	1 ± 2	65	23 ± 8	85	+	+
V32C	55 ± 26	66	50 ± 15	73	+	+
I33C	123 ± 37	68	184 ± 45	92	+	+
Cys-less GLUT1	82 ± 20	108	113 ± 19	147		

[a] *Xenopus* oocytes expressing a single-cysteine mutant were incubated at 21−22 °C for 30 min in Barth's medium containing 10 mM NEM or 1 mM pCMBS. In the presence of the sulfhydryl reagent, transport or uptake rates were assessed for tritium-labeled 3-OMG in the NEM group or 2-DOG in the pCMBS group. The uptake values of water-injected oocytes were always subtracted (for details, see Experimental Procedures). Transport activity in the presence of NEM or pCMBS was calculated from two to four separate experiments per mutant expressed as the percent uptake (mean ± the standard deviation) of that in the absence of the sulfhydryl reagent. Sensitivity (S) was jugded by statistically significant NEM-induced modification of 3-OMG transport and accessibility (A) by alteration of 2-DOG uptake induced by pCMBS. nd means no 3-OMG transport or 2-DOG uptake could be detected after subtraction of that of sulfhydryl reagent-treated water-injected *Xenopus* oocytes. The entries in the S column demonstrate significant transport alteration by NEM. A plus sign (+) indicates that the transport rate of a NEM-treated mutant is significantly different ($p < 0.01$) from those of both the untreated control and the NEM-treated Cys-less GLUT1. The entries in the A column indicate accessibility of residues to pCMBS. A plus sign (+) indicates that the uptake rate of a pCMBS-treated mutant is significantly different ($p < 0.01$) from those of both the untreated control and the pCMBS-treated Cys-less GLUT1, and an asterisk (*) indicates that the very low basal transport activity of a mutant transporter (<10% of the activity of Cys-less GLUT1) does not allow a definite classification.

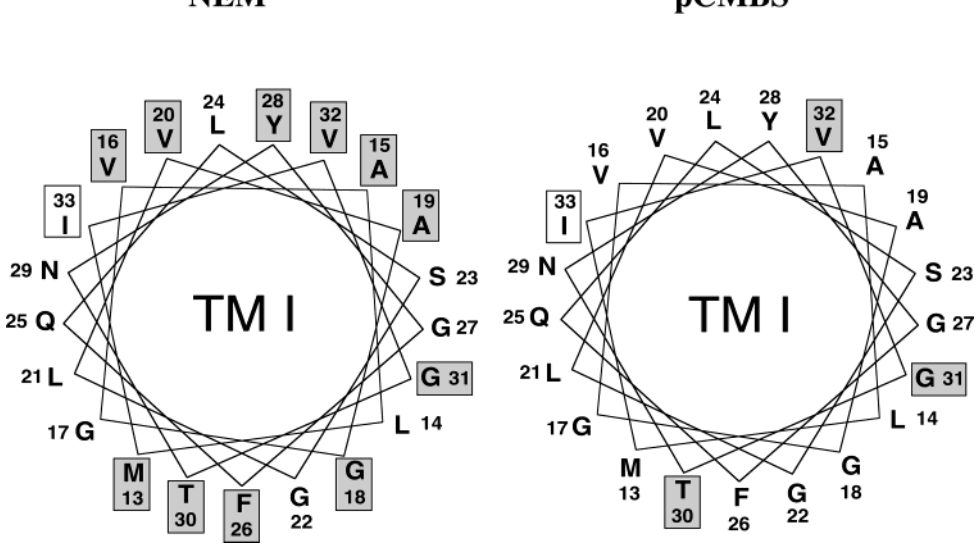

FIGURE 3: Helical wheel plot of amino acid residues in TM1 (presented in the one-letter code). Boxed positions indicate statistically significant ($p < 0.01$) effects by NEM on 3-OMG transport or by pCMBS on 2-DOG uptake. A gray background denotes inhibition, and a white background denotes stimulation. Single-cysteine mutants whose basal uptake rates were less than 10% of that of Cys-less GLUT1 (marked with asterisks in Table 2) were disregarded.

DISCUSSION

Basal Activities of Cysteine Replacement Mutants. Successive substitution of adjacent native amino acid residues with cysteine was previously applied to helices 2 (*13*), 5 (*14*), 7 (*13*, *15*), 10 (*16*), and 11 (*17*) of the cysteine-less GLUT1 glucose transporter. Cysteine scanning at TM1 indicated that the majority of the 21 single-cysteine mutants are functional. In seven single-cysteine mutants, whose relative transport activities were less than 50% of that of the Cys-less GLUT1, the native amino acid residues are identical or homologous in GLUT1−GLUT4, indicating the functional importance of their side chains. For some of the single-cysteine mutants (i.e., A19C, L21C, S23C, Q25C, and G27C), dot blot analysis and confocal microscopy suggested that reduced transport activities resulted from a reduced level of translation of injected mutant cRNAs and, on the basis of the ratio of plasma membrane to cytoplasm fluorescence intensities, from impaired plasma membrane targeting of the mutant transporter proteins. As reported for TM2, TM5, and TM11, the substitution-sensitive positions within TM1 with less than 50% of the activity of the single-cysteine mutant remaining are localized at the central part of the plasma membrane. This distribution pattern differed from that of TM10, where these substitution-sensitive positions are distributed at the cytoplasmic half of the plasma membrane. In TM7, these positions are distributed along the entire membrane thickness. If the replacement-sensitive positions within TM1 are presented as a helical wheel plot (not shown), they are located along a helix circumference comparable to the distribution pattern in helices 5, 7, and 10, which is different from helices 2 and 11, where these positions are preferentially concentrated on one side of the helix structure.

Sulfhydryl Group Sensitivity and Accessibility Scanning. Two sulfhydryl reagents, NEM and pCMBS, had been chosen to discriminate between cysteine residues that are sensitive to transport alteration by membrane-permeable sulfhydryl reagents such as NEM and those, identified by pCMBS accessibility, that form a water-accessible surface. pCMBS is a highly specific but reversible sulfhydryl reagent, whereas NEM forms a stable alkyl derivative (*29*). Alkylation of cysteine may inactivate the transport protein by blocking binding, introducing steric hindrance, or inducing alteration in the three-dimensional protein structure. The differential reactivity may be explained by the number of accessible SH groups according to differences in membrane permeability of the two agents. The factors which determine the indirect effects on cysteine-less GLUT1 remain unknown. Chemical modification of sulfhydryl-containing proteins interacting with the GLUT transporter may be a rational explanation. In addition, under special conditions (100 mM NEM and pH 6.4−7.4), histidine and histidine polypeptides can be acylated by NEM (*30*). The importance of this reaction with transport proteins, particularly at a concentration of 10 mmol/L, is not known. Fortunately, the majority of substituted cysteines that reacted with NEM led to transport modification (marked S+ in Table 2), mostly inhibition. In five cysteine mutants, the extremely low basal activities interfered with an assessment of NEM sensitivity (marked S* in Table 2). Moreover, cysteine substitution at positions L14, G17, L24, and N29 did not lead to transport modification after application of sulfhydryl reagents. These positions may be part of a local helix structure that is not important for conformational changes during glucose transfer through the membrane or may form a local structure that limits NEM access to these thiol-containing sites. Taken together, 12 of the 21 single cysteine residues were potential reporters of water-accessible positions for solutes from the external environment using pCMBS. Residues forming a water-accessible surface were at the exofacial end of the plasma membrane and were located along a helix circumference. Marginal basal transport activity (three mutants) or the lack of significant NEM sensitivity (two mutants) at the exofacial half of the plasma membrane was an obstacle to the unequivocal identification of further pCMBS-sensitive positions. In all transmembrane segments that have been investigated except for TM10 (*16*), the pCMBS-accessible cysteine residues are concentrated at

the exofacial half of the plasma membrane and, in contrast to the circumferential distribution within TM1 or TM7, cluster at one side of the helix. On the basis of the recently published substantial three-dimensional GLUT1 model (10), TM1 may participate in the formation of an auxiliary pore for solutes other than glucose.

Two *Escherichia coli* transporters, the lactose permease (LacY) and the glycerol 3-phosphate transporter (GlpT), have been crystallized recently (*11*, *12*). The X-ray structures represent both transporters in the inward-facing conformation in the presence (LacY) or absence (GlpT) of a substrate. As reported for GLUT1 and most MFS proteins, they have 12 transmembrane α-helices with both the N- and C-terminal domains located in the cytoplasm. Consistent with all published GLUT1 membrane topology models, two distinct groups of six helices are connected by a long loop between helices 6 and 7. With regard to the role of TM1 in helix packing and pore formation, the *E. coli* lactose permease builds a hydrophilic cavity that is formed between helices 1, 2, 4, and 5 of the N-terminal half and helices 7, 8, 10, and 11 of the C-terminal half (*11*). In the GlpT crystal structure, the substrate translocation pore is lined by four central helices, i.e., helices 1, 4, 7, and 10, and by peripheral helices 2, 5, 8, and 11. Helix 1, containing 38 amino acids, extends beyond the membrane boundary on the cytoplasmic side (*12*). According to the secondary structure of GLUT1 (*4*), 21 amino acids of TM1 have been addressed by cysteine-scanning mutagenesis. The presented data indicate that the exofacial part of the helix is exposed to the solvent. This fits with a model where helix 1, as shown for both bacterial transporters, is integrated in a pore-forming helical bundle. An extension of cysteine-scanning mutagenesis toward the N-terminus of GLUT1 is not expected to add further information about extracellular solute accessibility. Both crystal structures do not indicate a second channel as proposed for the multifunctional GLUT1 (*10*).

REFERENCES

1. Marger, M. D., and Saier, M. H. (1993) *Trends Biochem. Sci. 18*, 13−20.
2. Joost, H. G., and Thorens, B. (2001) *Mol. Membr. Biol. 18*, 247−256.
3. Goswitz, V. C., and Brooker, R. J. (1995) *Protein Sci. 4*, 534−537.
4. Mueckler, M., Caruso, C., Baldwin, S. A., Panico, M., Blench, I., Morris, H. R., Allard, W. J., Lienhard, G. L., and Lodish, H. F. (1985) *Science 229*, 941−945.
5. Baldwin, S. A. (1993) *Biochim. Biophys. Acta 1154*, 17−49.
6. Gould, G. W., and Holman, G. D. (1993) *Biochem. J. 295*, 329−341.
7. Zeng, H., Parthasarathy, R., Rampal, A. L., and Jung, C. Y. (1996) *Biophys. J. 70*, 14−21.
8. Widdas, W. F. (1998) *Exp. Physiol. 83*, 187−194.
9. Hruz, P. W., and Mueckler, M. M. (2001) *Mol. Membr. Biol. 18*, 183−193.
10. Zuniga, F. A., Shi, G., Haller, J. F., Rubashkin, A., Flynn, D. R., Iserovich, P., and Fischbarg, J. (2001) *J. Biol. Chem. 276*, 44970−44975.
11. Abramson, J., Smirnova, I., Kasho, V., Verner, G., Kaback, H. R., and Iwata, S. (2003) *Science 301*, 610−615.
12. Huang, Y., Lemieux, M. J., Song, J., Auer, M., and Wang, D.-N. (2003) *Science 301*, 616−620.
13. Olsowski, A., Monden, I., Krause, G., and Keller, K. (2000) *Biochemistry 39*, 2469−2474.
14. Mueckler, M., and Makepeace, C. (1999) *J. Biol. Chem. 274*, 10923−10926.
15. Hruz, P. W., and Mueckler, M. M. (1999) *J. Biol. Chem. 274*, 36176−36180.
16. Mueckler, M. M., and Makepeace, C. (2002) *J. Biol. Chem. 277*, 33498−33503.
17. Hruz, P. W., and Mueckler, M. M. (2000) *Biochemistry 39*, 3967−3972.
18. Karlin, A., and Akabas, M. H. (1998) *Methods Enzymol. 293*, 123−145.
19. Due, A. D., Cook, J. A., Fletcher, S. J., Zhi-Chao, Q., Powers, A. C., and May, J. M. (1995) *Biochem. Biophys. Res. Commun. 208*, 590−596.
20. Wellner, M., Monden, I., and Keller, K. (1995) *FEBS Lett. 370*, 19−22.
21. Mueckler, M., and Makepeace, C. (1997) *J. Biol. Chem. 272*, 30141−30146.
22. Mueckler, M., and Lodish, H. F. (1986) *Cell 44*, 629−637.
23. Krieg, P. A., and Melton, D. A. (1984) *Nucleic Acids Res. 14*, 7057−7070.
24. Keller, K., Strube, M., and Mueckler, M. (1989) *J. Biol. Chem. 264*, 18884−18889.
25. Garcia, J. C., Strube, M., Leingang, K., Keller, K., and Mueckler, M. (1992) *J. Biol. Chem. 267*, 7770−7776.
26. Wellner, M., Monden, I., Mueckler, M., and Keller, K. (1995) *Eur. J. Biochem. 227*, 454−458.
27. Monden, I., Olsowski, A., Krause, G., and Keller, K. (2001) *Biol. Chem. 382*, 1551−1558.
28. D'Amore, T., and Lo, T. C. Y. (1986) *J. Cell. Physiol. 127*, 106−113.
29. Riordan, J. F., and Vallee, B. L. (1972) *Methods Enzymol. 25*, 449−456.
30. Webb, J. L. (1966) in *Enzyme and Metabolic Inhibitors*, Vol. III, pp 337−365, Academic Press, New York.

BI030175W